The Use of Ultrasonics for Nano-emulsion Preparation

S.Kentish[1*], T. Wooster[2], M. Ashokkumar[1], S. Balachandran[1], R. Mawson[2], L. Simons[2]

[1]Particulate Fluids Processing Centre, School of Chemistry/Department of Chemical and Biomolecular Engineering, University of Melbourne, Victoria 3010
[2]Food Science Australia, 671 Sneydes Road, Werribee, VIC 3030, Australia

[*]Corresponding Author: sandraek@unimelb.edu.au,
Tel: +61 3 8344 6683, Fax: +61 3 8344 4153

Abstract

Oil in water emulsions are an important vehicle for the delivery of hydrophobic bioactive compounds into a range of food products. The preparation of very fine emulsions is of increasing interest to the beverage industry, as novel ingredients can be added with negligible impact to solution clarity. In the present study, both a batch and focused flow-through ultrasonic cell were utilized for emulsification with ultrasonic power generation at 20 - 24 kHz. Emulsions with a mean droplet size as low as 135 ± 5 nm were achieved using a mixture of flaxseed oil and water in the presence of Tween 40 surfactant. Results are comparable to those for emulsions prepared with a microfluidizer operated at 100 MPa. The key to efficient ultrasonic emulsification is to determine an optimum ultrasonic energy intensity input for these systems, as excess energy input may lead to an increase in droplet size.

Keywords: Ultrasound, emulsion, triglyceride, surfactant

Industrial Relevance:

The preparation of oil in water emulsions is a common feature of food processing operations. The use of ultrasound for this purpose can be competitive or even superior in terms of droplet size and energy efficiency when compared to classical rotor-stator dispersion. It may also be more practicable with respect to production cost, equipment contamination and aseptic processing than a microfluidisation approach. The present paper shows that ultrasound can be

effective in producing nano-emulsions for use in a range of food ingredients.

Introduction

Food grade emulsions formed from oils rich in Omega-3 polyunsaturated fatty acids (PUFA), such as fish oil and flax seed oil are commercially attractive because of the potential health benefits associated with their consumption (Burdge & Calder 2006; Kolanowski & Laufenberg 2006). Flax seed oil has the extra benefit of a pleasant odor compared to fish oil (Burdge & Calder 2006). The preparation of such emulsions with small droplet size is of particular interest. Small droplet sizes in general leads to a creamier mouth feel and greater emulsion stability (McClements, 2004). Furthermore, reductions in oil droplet sizes below 100 nanometres have the potential to provide a translucent emulsion (Tadros, Izquierdo, Esquena & Solans, 2004) that can be incorporated readily into beverages and food gels without loss of opacity. There are a number of mechanisms available for the production of such emulsions. The traditional method employed in the food industry uses valve homogenization (McClements, 2004). This process is energy intensive as only a small percentage of the applied energy is effective (Tadros et al. 2004). Since the mid 1990's a high energy emulsification device, a microfluidizer, has gained prevalence (McClements, 2004; Strawbridge, Ray, Hallett, Tosh & Dalgleish, 1995). This technique uses particle-particle collision through a microfluidic channel architecture rather than a straight shear field, to cause particle size reduction (McClements, 2004).

The use of low frequency ultrasound for emulsion formation is well established, at least on a laboratory scale (Richards, 1929; Abismail, Canselier, Wilhem, Delmas & Gourdon 1999) However, most work to date has focused on the preparation of synthetic emulsions, for example for the paint industry or in the preparation of polymeric nano-particles. The development of such techniques for the food industry is a much more recent phenomenon (Freitas, Hielscher, Merkle & Gander, 2006; Jafari, He & Bandari, 2006).

Ultrasonic emulsification is believed to occur through two mechanisms. Firstly, the application of an acoustic field produces interfacial waves which become unstable, eventually resulting in the eruption of the oil phase into the water medium in the form of droplets (Li & Fogler 1978a). Secondly, the application of low frequency ultrasound causes acoustic cavitation, that is, the formation and subsequent collapse of microbubbles by the pressure fluctuations of a simple sound wave. Each bubble collapse (an implosion on a microscopic scale) event causes extreme levels of highly localised turbulence. The turbulent micro-implosions act as a very effective method of breaking up primary droplets of dispersed oil into droplets of sub-micron size (Li & Fogler 1978b).

Studies to date comparing ultrasonic emulsification with rotor-stator dispersing have found ultrasound to be competitive or even superior in terms of droplet size and energy efficiency (Ma & Hsu 1999, Abismail et al., 1999, Tadros et al. 2004). Microfluidization has been found to be more efficient than ultrasound, but less practicable with respect to production cost, equipment contamination and aseptic processing (Abismail et al., 1999). Comparing mechanical agitation to ultrasound at low frequency, Tadros et al. (2004) found that for a given desired diameter, the surfactant amount required was reduced, energy consumption (through heat loss) was lower and the ultrasonic emulsions were less polydispersed and more stable. It is the purpose of the present paper to further investigate the usefulness of ultrasound to generate food grade oil-water nano-emulsions and in particular to identify equipment-related constraints.

Materials and Methods

All base emulsions were prepared from unrefined organically grown cold pressed flax seed oil (long chain triglyceride oil) as supplied by Stoney Creek (Victoria, Australia) and reagent grade Tween 40 (C16), as supplied from Sigma Aldrich (Sydney, Australia). Unless otherwise stated, the emulsion formulation was 15 vol% flaxseed oil, 5.6 vol% Tween 40 and 79.4 vol% deionised water.

Two ultrasonic experimental set-ups were utilised. Batch experiments employed a Branson Sonifier of nominal power 400W and frequency 20 kHz with a 19mm diameter tip horn. This was placed in a custom-built cylindrical glass cell of internal diameter 60 mm with in-built cooling jacket. Chilled water at 3.5 C was passed continuously through this jacket. For each experiment, emulsion samples of either 30, 50 or 75 ml total volume were prepared and pre-mixed at 13,500 rpm with an Ultra-turrax mixer for 2 minutes. The droplet size after pre-mixing was very broad, exhibiting three modes at droplet sizes 0.13, 1.0 and 5.0 μm, and a volumetric mean size of 0.4 ± 0.5 μm. The samples were then placed in the glass cell. The sonifier tip horn was adjusted until it was 2 cm below the surface of a 75 ml sample or 1cm below the surface of a 30 or 50ml sample.

The second series of experiments used a focussed flow through cell powered by a 400S Hielscher Sonifier of 400W nominal power and frequency 24 kHz equipped with a 22 mm sonotrode tip (Figure 1) and flow cell chamber of 5.6 ml. In this case, the emulsions were pre-homogenised with a Silverson rotor-stator mixer to a mono-modal droplet size distribution of average 6.4 ± 0.3 μm and then pumped through the cell using a Micropump Model 180 (USA),

supplied by Process Pumps (Australia). Flowrates through the cell were varied from 20 to 110 m mL.min^{-1}, giving residence times of 3 to 19 seconds.

Emulsions were also prepared using a Microfluidics M-110Y microfluidizer (MFIC Corporation, Newton, MA, USA) with a F20 Y 75 μm interaction chamber and H30 Z 200 μm auxiliary chamber inline. Emulsions were prepared by subjecting pre-emulsions to 5 passes (unless otherwise stated) at 100 MPa. Pre-emulsions were prepared using a Silverson rotor-stator mixer on its lowest speed setting for 2 minutes and had a average particle size $D_{3,2}$ of 8.37 ± 0.025 μm in a mono-modal distribution. The initial temperature of the pre-emulsion was room temperature, however processing of the emulsions increased the temperature to 50-60^{o}C.

Emulsion particle size was assessed by laser light scattering using a Mastersizer 2000 (Malvern, Worcestershire, United Kingdom). Samples were diluted to approximately 0.002 wt%, in an effort to avoid multiple scattering effects. Information about emulsion particle size was then obtained via a best fit between light scattering (Mie) theory and the measured particle size distribution. A refractive index of 1.48 and absorption of 0.02 was used for flax seed oil in Mie theory calculations. Emulsion particle sizes are of the volume – length mean diameter $d_{4,3}$ ($d_{4,3} = \Sigma n_i d_i^4 / \Sigma n_i d_i^3$). Emulsion particle size results are an average of three measurements and are quoted as the volume-surface mean diameter $d_{3,2}$ ($d_{3,2} = \Sigma n_i d_i^3 / \Sigma n_i d_i^2$).

The ultrasonic energy transferred into the emulsion was measured calorimetrically by observing the temperature change of a similar volume of water with time (Kimura et al. 1996; Ratoarinoro, Contamine, Wilhelm, Berlan & Delmas 1995).

Results and Discussion

The size of an emulsion droplet formed by homogenization is controlled by the interplay between droplet breakup and droplet coalescence (Tadros et al. 2004; McClements, 2004). Droplet break up is controlled by the type and amount of shear applied to droplets as well as the droplets resistance to deformation (Laplace pressure) which is determined by the surfactant (Tadros et al. 2004; McClements, 2004). The rate of droplet coalescence (related to droplet stability) is determined by the ability of the surfactant to rapidly adsorb to the surface of newly formed droplets; this is governed by surfactant surface activity and concentration (Tadros et al. 2004; McClements, 2004).

In the present study Tween 40 was used as the surfactant and the effect of its concentration can be seen in Figure 2. The relationship between emulsion particle size and Tween content can be explained in terms of surfactant surface coverage. At low Tween contents there is insufficient surfactant, newly formed droplets coalesce and the emulsion droplet size is determined by the surfactant concentration. Initially increasing surfactant concentration results in a large decrease in particle size because more surfactant is able to stabilize the newly formed droplets. Once there is an excess of surfactant, about 2% Tween, the rate of the decrease in emulsion droplet size with increasing surfactant concentration decreases. This is because the concentration of surfactant in the bulk is sufficient to allow rapid diffusion and adsorption of the surfactant to newly formed droplets. Any further increase in surfactant concentration only leads to a small increase in surfactant diffusion and hence a small decrease in droplet coalescence. In the present system it appears that a Tween content of about 5 to 7 wt% is close to the limit of the decrease in particle size. Therefore Tween concentrations at this level were used in all subsequent studies. While this may appear to be a relatively large amount of surfactant, the flaxseed emulsions under study in

this paper are likely to be added in only very small quantities to other food substances and hence the total amount of surfactant provided to the consumer will be small.

Residence Time and Input Power

Batch experiments were initially conducted to examine the effect of power intensity, pre-emulsification and sonication time. As shown in Figure 3, a total sonication time of five minutes was found to produce optimum results, with additional sonication providing no greater reduction in droplet size.

The effect of applied power was next considered. Conventionally it would be expected that the amount of shear would increase with the applied power, the emulsion particle size should then decrease with increasing shear. However the results shown in Figure 4, demonstrate that the droplet size passes through a minimum size at an intermediate power application and then increases at higher power levels. A similar trend between emulsion particle size and applied shear has been observed by others for emulsions made with proteins and/or modified starches (Desrumaux & Marcand 2002; Jafari et al. 2006; Tornberg 1980). In these studies the effect has been described as “over-processing” which is caused by an increase in emulsion droplet coalescence at the higher shear rates (Desrumaux et al. 2002; Jafari et al. 2006; Tornberg 1980). In the present case, ultrasonic radiation forces (referred to as Bjerknes forces (Leighton 1994)) will increase in intensity as applied power increases. The secondary Bjerknes force will drive emulsion droplets to the nodes and antinodes of the acoustic field. The closer proximity of the droplets at these positions would result in increased droplet coalescence and hence the observed “over-processing” (Pangu & Feke, 2004).

Alternatively, the conversion of input power to delivered power is less efficient at the higher power levels and this will affect results. Figure 5 shows this relationship between input and delivered power as measured by the temperature increase in the cell over time. The results cover a range of sample volumes with a small sample volume corresponding to a large power density. The results also compare the effect of a pitted horn tip with a polished tip that would again deliver greater power density. It is evident from Figure 5 that as the power density increases; the conversion of this input power into delivered power reduces. This inability for the horn to transfer energy into the solution at high power densities is a well known phenomenon. As the power density increases, the production of acoustic bubbles increases in the area below the horn. Indeed, these bubbles will collect at the nodes of the acoustic field through the same Bjerknes forces as described above. This bubble cloud shields the remainder of the solution from the ultrasonic energy source and hence power transmission decreases.

An experiment was also conducted in the batch cell where the pre-emulsification step was omitted. An identical droplet size distribution was obtained, indicating that such pre-mixing is not required to produce a nano-emulsion with ultrasound. However, pre-mixing will always be required in a continuous flow-through arrangement to ensure that a consistent emulsion formulation can be pumped into the cell.

In the focused flow through cell, a series of 48 experiments were conducted over a range of nominal input powers (80 to 210 W) and pump speeds (20 to 110 $mL.min^{-1}$). These results were analysed by multiple linear regression. Table 1 summarizes the results of this regression analysis while a selection of this data and the model curve resulting from the regression analysis is presented in Figure 6. This analysis showed similar trends as in the batch cell, that is, a decline in

droplet size as residence time increases (pump speed decreases) and a power input level beyond which droplet coalescence and bubble cloud blanketing of the horn prevents further decreases in droplet size.

While it was not possible to increase the residence time in the flow through cell by further reducing the pump flow rate, this residence time could be increased by recirculating the emulsion so that it passed through the cell more than once. Gains from multiple passes were incremental, with the surface average mean diameter reducing only from 0.14 to 0.13 micron when the number of passes was increased from one to three at an input power of 340 W and a pump flow rate of 20 $mL.min^{-1}$ (residence time per pass of 17 seconds) (Figure 7). While this represents a 24% increase in the number of droplets, it requires a 300% increase in energy consumption. Further increases in the number of passes had no effect. This suggests that in the flow through arrangement increments in residence time beyond around one minute are ineffective.

Also shown in Figure 7 is comparable data obtained using a microfluidisation device. It is clear that the two devices produce similar results. In fact the ultimate difference between ultrasound and microfluidisation is much smaller than other researchers have found using a 24 kHz horn sonicator (Jafari, He & Bhandari 2006). This is important because a preliminary analysis of the energy requirements suggest that ultrasound may be a more cost effective processing option. It should however be noted that this comparison is valid only for the emulsions considered in this paper. The two devices are likely to produce different results with other formulations, depending on the surface energy and viscosity of the system.

Overall, the minimum droplet size produced in either the batch or flow through sonication cell with the emulsion formulation described was 0.12 micron (obtained in a 50ml sample size batch run at 200 W nominal power). This droplet size is significantly below that recently reported by Freitas et al. (2006) for comparable food grade emulsions generated by ultrasound (0.4 – 0.6 micron). Further, results showed that emulsions produced by either the batch or flow through cell were shelf stable for a period of at least twelve days.

Equipment Design Issues

While batch experiments are useful for laboratory studies, continuous flow equipment will almost always be required in an industrial size application. A major challenge for the introduction of ultrasonic technology is the effective design of such flow through equipment. In particular, it is essential that in such devices, all elements of the fluid experience similar levels of ultrasonic power intensity. With the present flow through cell, it was apparent that a fraction of the fluid flow bypassed the 'hot zone' of the ultrasonic horn tip, as evidenced by a shoulder in the droplet size distribution at higher droplet sizes (see Figure 8). One of the major aims of our ongoing work is to develop better equipment designs that eliminate such effects.

A further concern for the commercial application of this technology is that when a standard titanium ultrasonic horn tip is used, titanium ions or particles can be emitted into the product by cavitational abrasion of the sonotrode (Freitas et al. 2006). A further focus of our ongoing work is the development of equipment designs where the ultrasonic transducer is physically separated from the process fluid by an abrasion resistant barrier. This will be essential for food grade applications.

Conclusions

A range of food grade emulsions have been prepared from a flaxseed oil/water mixture. Results show that there is an optimum power input level beyond which droplet coalescence and cavitational bubble cloud formation restricts performance. Increasing residence time reduces droplet sizes to a point, but continued sonication beyond one to five minutes is ineffective. While the batch cell produces better results, continuous equipment is likely to be more viable in a commercial environment. In order to achieve such a commercial outcome, significant additional work is required to optimize equipment design. Bypassing of fluid around the ultrasonic 'hot zone' must be minimized and designs developed where transducer tip erosion does not contaminate process fluids.

Acknowledgements

Funding for this project was partially provided by the University of Melbourne-CSIRO Collaborative Research Support Scheme. Some infrastructure funding was also provided by the Victorian government through a Science Technology and Innovation Infrastructure Grant. This financial assistance is gratefully acknowledged.

References

Abismail B., Canselier J., Wilhelm A., Delmas H., & Gourdon C. (1999). Emulsification by ultrasound: drop size distribution and stability. *Ultrasonics Sonocheistry*, 6, 75-83.

Burdge, G.C., & Calder, P.C. (2006) Dietary alpha-linolenic acid and health-related Outcomes: a metabolic perspective. *Nutrition Research Reviews*, 19, 26-52.

Desrumaux, A., & Marcand, J. (2002) Formation of sunflower oil emulsions stabilized by whey proteins with high-pressure homogenization (up to 350 Mpa): effect of pressure on emulsion characteristics. *International Journal of Food Science and Technology*, 37, 263-269.

Freitas S., Hielscher G., Merkle H., & Gander B. (2006). Continuous contact- and contamination-free ultrasonic emulsification—a useful tool for pharmaceutical development and production. *Ultrasonics Sonochemistry*, 13, 76-85.

Jafari, S. M., He, Y., & Bhandari, B., (2006) Nano-Emulsion Production by Sonication and Microfluidization—A Comparison, *International Journal of Food Properties*, 9, 475-485.

Kimura T., Sakamoto T., Leveque J.-M., Sohmiya H., Fujita M., Ikeda S., & Ando T., (1996). Standardization of ultrasonic power for sonochemical reaction, *Ultrasonics Sonochemistry*, 3 (3) S157-S161.

Kolanowski, W., & Laufenberg, G., (2006) Enrichment of food products with polyunsaturated fatty acids by fish oil addition. *European Food Research and Technology*, 222, 472-477.

Leighton T.G., (1994) *The Acoustic Bubble* Academic Press, London.

Li M.K., & Fogler H.S., (1978a) Acoustic emulsification. Part 1. The instability of the oil-water interface to form the initial droplets *Journal of Fluid Mechanics*, 88(3), 499-511.

Li M.K., & Fogler H.S., (1978b) Acoustic emulsification. Part 2. Break-up of the larger primary oil droplets in a water medium, *Journal of Fluid Mechanics*, 88(3), 513-528.

296 Ma Y.F., Hsu C.C., (1999) Performance of sonication and microfluidization for liquid–liquid
297 emulsification, *Pharmaceutical Development And Technology* 4 233–240.
298 McClements D.J. (2004) *Food Emulsions: Principles, Practices, and Techniques*, 2nd edition,
299 CRC Press, Boca Raton, Florida.
300 Pangu, G. D., & Feke, D. L. (2004) Acoustically aided separation of oil droplets from aqueous
301 emulsions. *Chemical Engineering Science* 59(15), 3183-3193.
302 Ratoarinoro F., Contamine, Wilhelm A.M., Berlan J., & Delmas H., (1995) Power measurement
303 in sonochemistry, *Ultrasonics Sonochemistry*, 2(1), S43-S47.
304 Richards W.T., (1929) The chemical effects of high frequency sound waves I. A study of
305 emulsifying action *Journal of the American Chemical Society*, 51, 1724–1729.
306 Strawbridge K. B., Ray, E., Hallett F. R., Tosh S. M., & Dalgleish, D. G., (1995) Measurement
307 of particle size distributions in milk homogenized by a microfluidizer: estimation of
308 populations of particles with radii less than 100 nm. *Journal of Colloid and Interface*
309 *Science*, 171, 392 - 8.
310 Tadros T., Izquierdo P., Esquena J., & Solans C. (2004). Formation and stability of nano-
311 emulsions. A*dvances in Colloid and Interface Science*, 108-109, 303-318.
312 Tornberg, E. (1980) Functional characteristics of protein stabilised emulsions: emulsifying
313 behaviour of proteins in a sonifier. *Journal of Food Science*, 45, 1662-1668.
314
315
316

Table Caption

Table 1 – Summary of statistical parameters arising from a multiple linear regression of the Sauter mean diameter droplet size obtained using the flow through cell.

Figure Captions

Figure 1 – Diagram of the focussed flow-through ultrasonic cell used for the preparation of nano-emulsions. The cell is equipped with a 22 mm sonotrode tip and flow cell chamber of 5.6 ml and was powered by a 400S Hielscher Sonifier of 400W nominal power and frequency 24 kHz.

Figure 2 – The effect of Tween 40 content on the particle size of 15 vol% flax seed oil-in-water prepared by microfluidisation (5 passes at 100 MPa). Error bars are based on two standard deviations, calculated from triplicate measurements on two samples.

Figure 3 – The effect of sonication time for a 50ml sample in the batch cell. Nominal ultrasonic power was 200W. Error bars are based on two standard deviations, calculated from seven pairs of replicate points.

Figure 4 – The effect of nominal applied power in the batch cell. (a) 50 ml Sample Size (b) 75 ml Sample Size. Error bars are based on two standard deviations, calculated from eight replicate unsonicated samples.

Figure 5 – Power calibration results in the batch cell across a range of sample volumes. The 75ml sample sizes compare a freshly polished horn (unpitted) with a horn tip that has become pitted on the surface and will thus deliver less power. Each power calibration was determined from the measurement of solution temperature at three points in time. The average standard percentage error of the subsequent linear regression of the temperature/time relationship was used to generate the error bars.

Figure 6 – Experimental data obtained with the focused flow through cell at a pump speed of 60 $mL.min^{-1}$ corresponding to a residence time of 5.6 seconds (symbols). Model curves resulting from multiple linear regression of the full experimental data set (solid lines) are also shown.

Figure 7 – A comparison of ultrasonic emulsification to microfluidisation. Particle size is shown as a function of the number of passes through each device. Ultrasonic results were obtained at 330W nominal power and a pump speed of 20 $mL.min^{-1}$ (residence time of 17 seconds per pass), with error bars generated from five pairs of replicate points.

Figure 8 – A comparison of results obtained with the batch and flow through cell. Batch results were obtained after 25 minutes sonication at 280W nominal input power. Flow through cell results were obtained after a single pass at 350W nominal power and a pump speed of 20 $mL.min^{-1}$ (residence time of 17 seconds).

352 Table 1

353

Coefficient of Variation (R^2)	63%			*F statistic*		24.7
Standard Error	0.032			*Probability of occurring by chance based on F statistic*		1.6×10^{-9}
Observations	48					
	Regression Coefficients	*Standard Error*	*t Statistic*	*Probability Value*	*95% Confidence Interval based on t-statistic*	
					Lower	*Upper*
Intercept	0.51	0.072	7.0	1.2×10^{-8}	0.36	0.65
Pump Speed ($mL.min^{-1}$)	0.0014	0.00027	5.1	5.9×10^{-06}	0.00084	0.0019
Power(W)	-0.0044	0.00099	-4.4	5.9×10^{-05}	-0.0064	-0.0024
Power^2(W^2)	1.2×10^{-05}	3.4×10^{-06}	3.7	0.00061	5.64×10^{-06}	1.92×10^{-05}

354

355

356 Figure 1

357

358

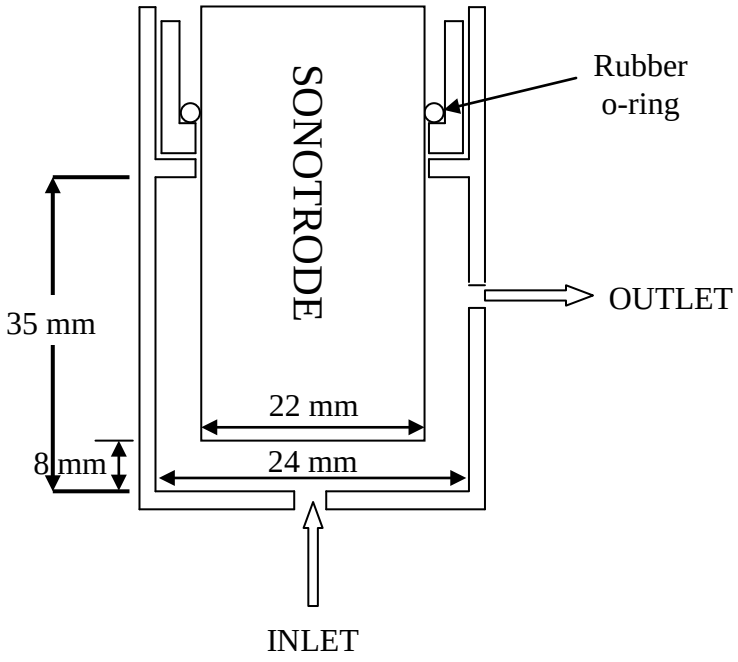

359 Figure 2

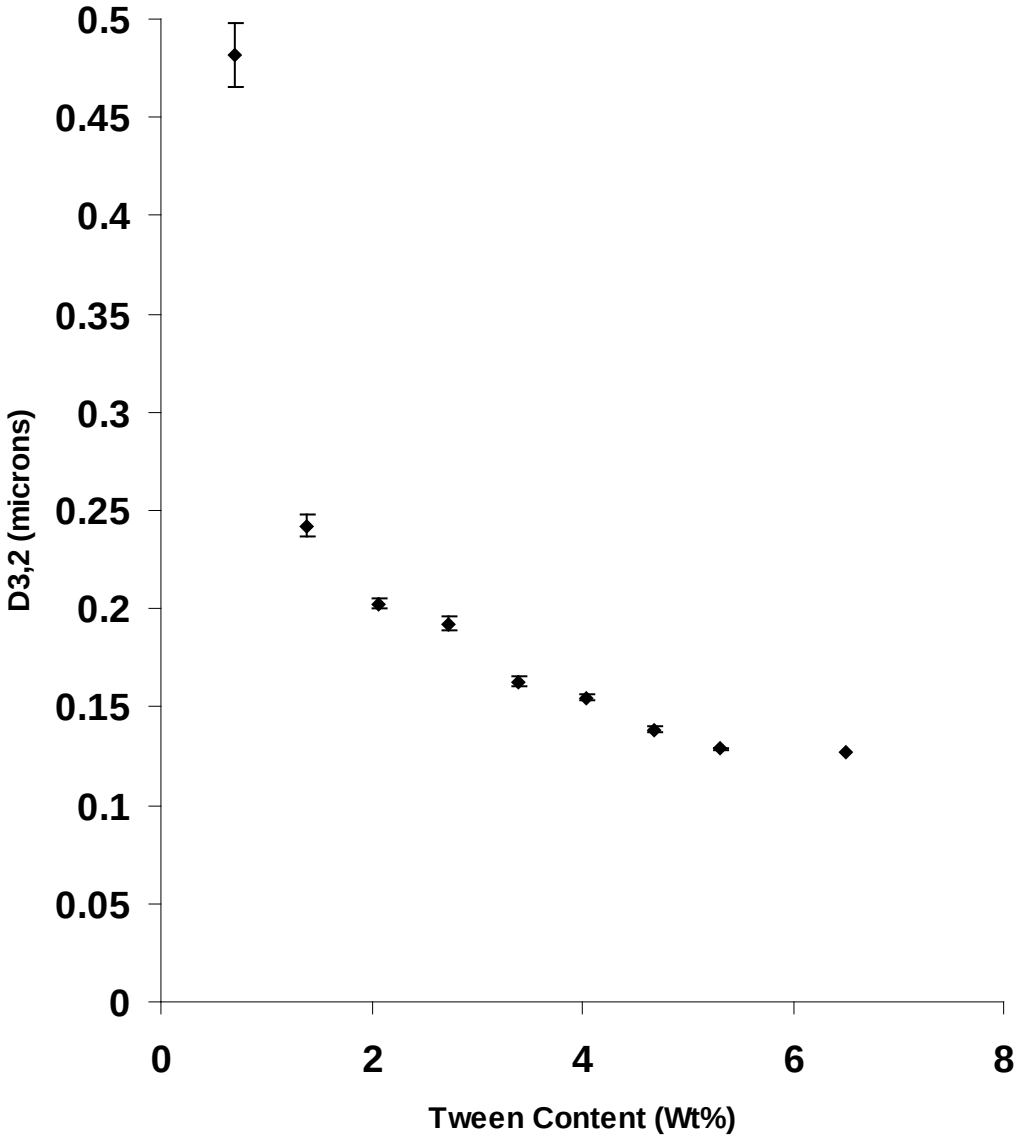

360

361 Figure 3

362

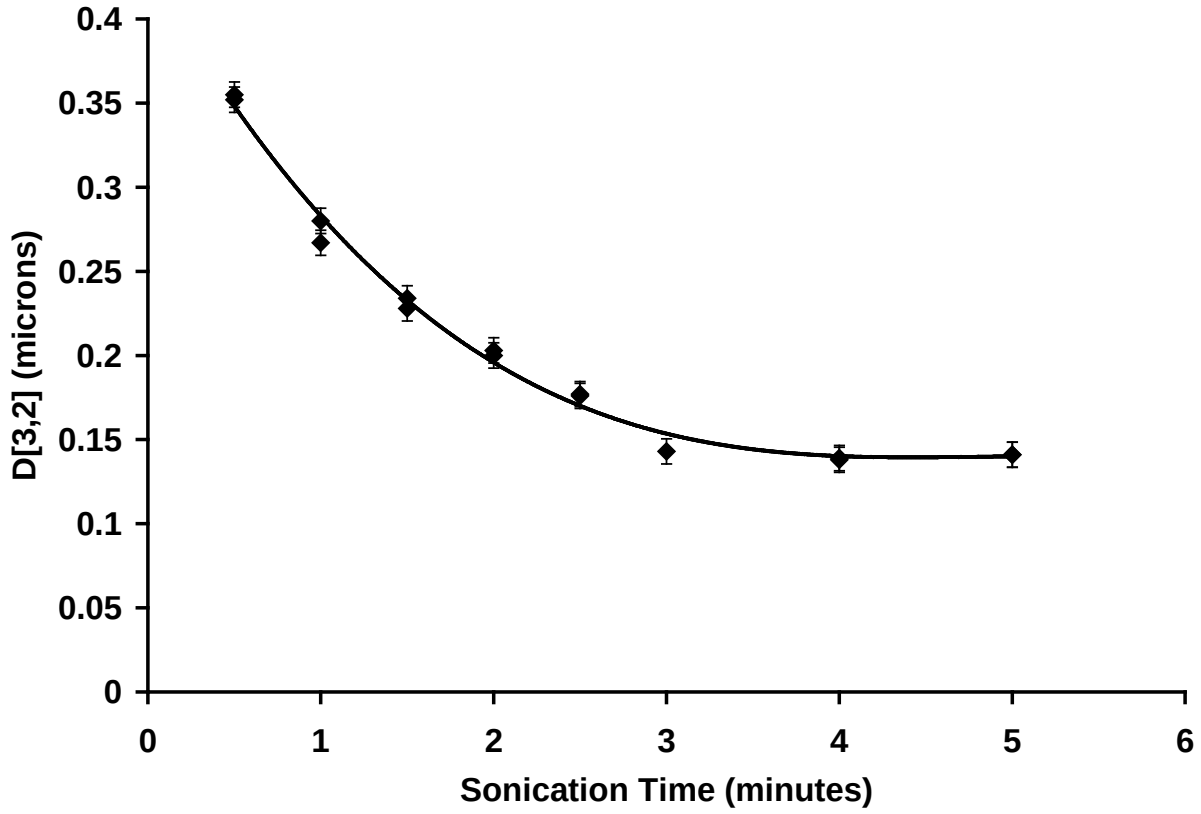

363

364

365

Figure 4

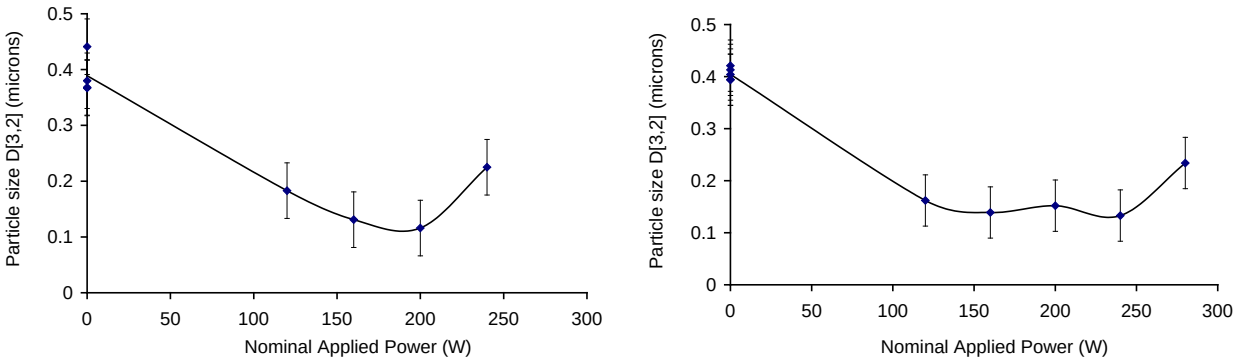
Particle size D[3,2] (microns)
0.5
0.4
0.3
0.2
0.1
0
0
50
100
150
200
250
300
Nominal Applied Power (W)
Particle size D[3,2] (microns)
0.5
0.4
0.3
0.2
0.1
0
0
50
100
150
200
250
300
Nominal Applied Power (W)

377 Figure 5

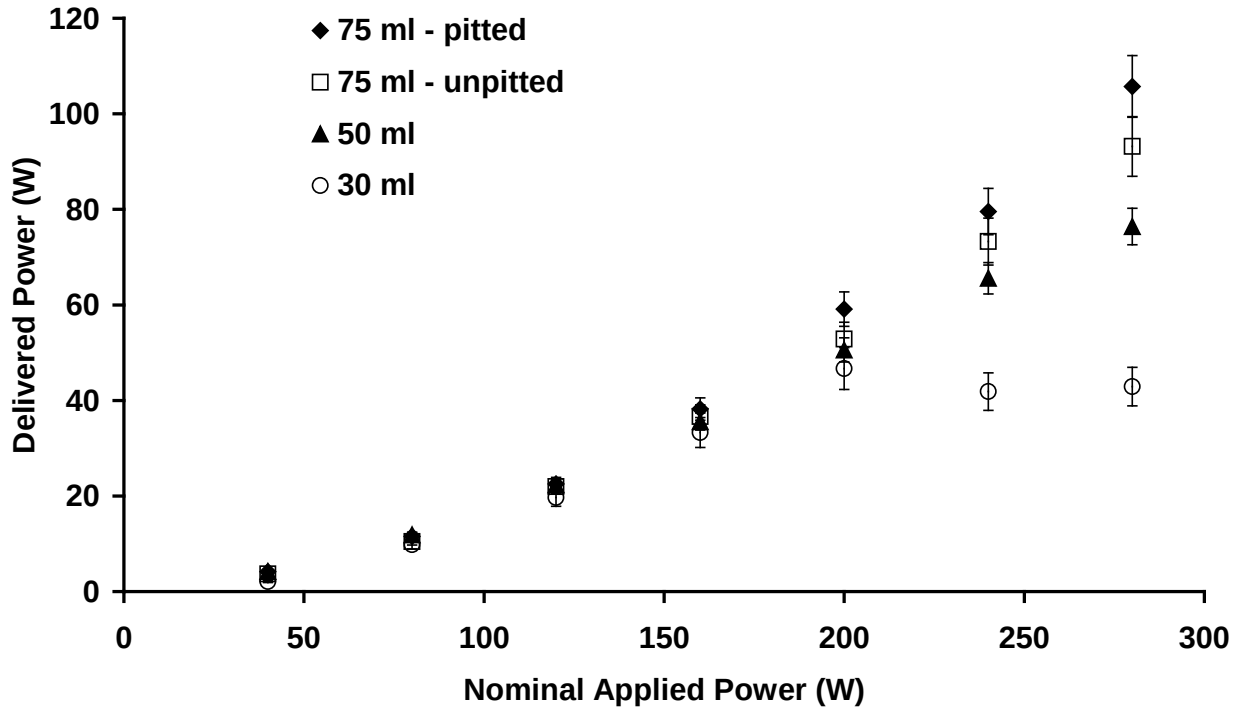

378

379

380

381

382

383

384

385

386

387 Figure 6

388

389

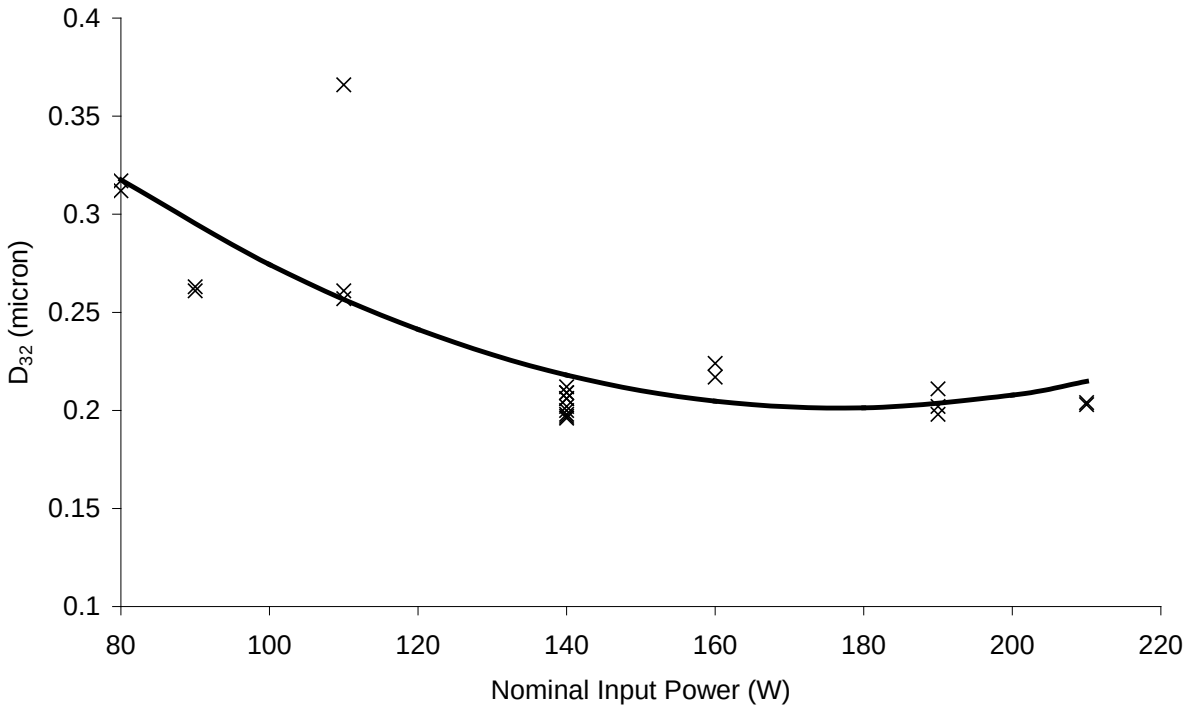

390 Figure 7

391

392

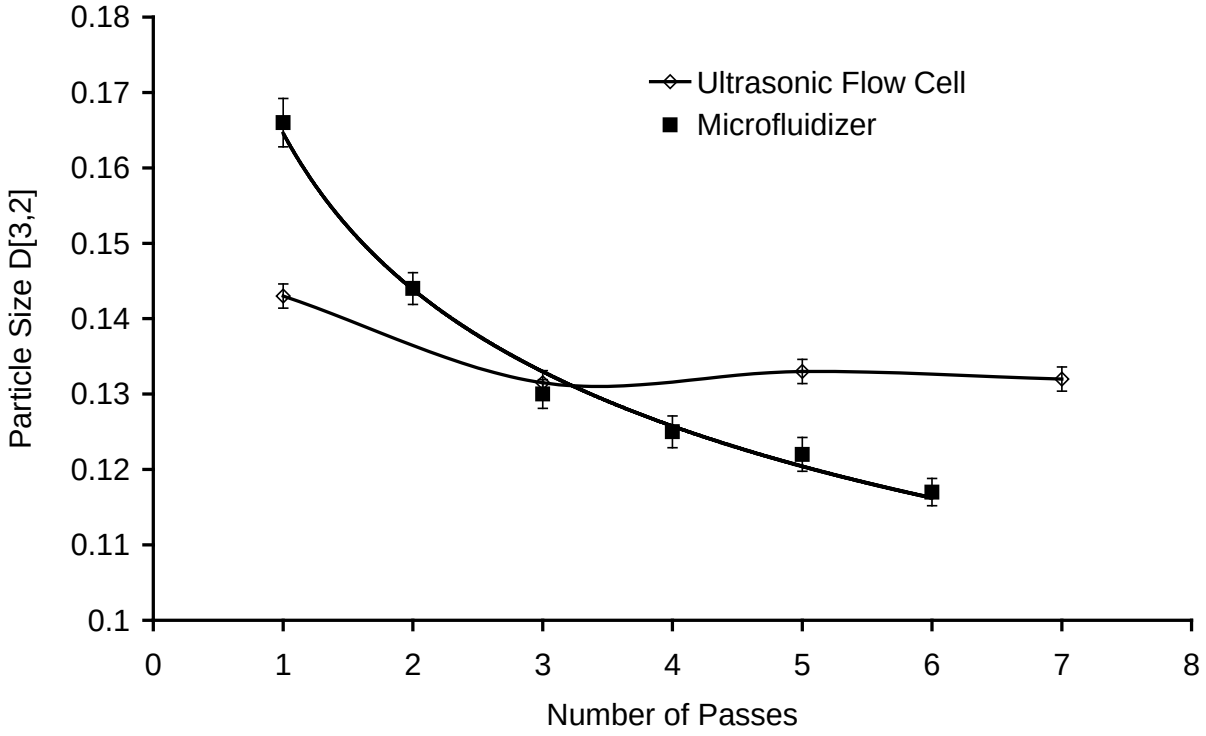

393

394

395 Figure 8

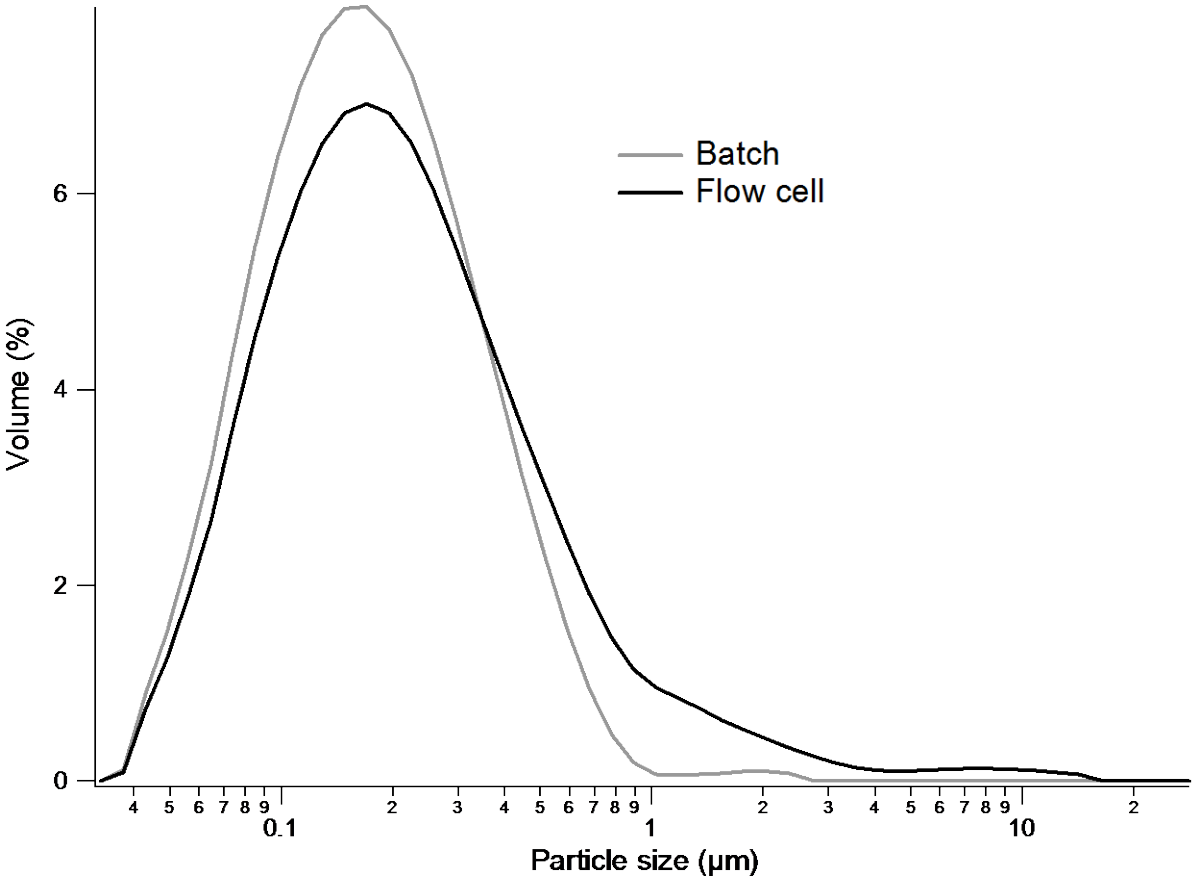

396

397

398